Zeno and anti-Zeno effects in spin-bath models

Dvira Segal and David R. Reichman
Department of Chemistry, Columbia University, 3000 Broadway, New York, New York 10027, USA
(Received 23 January 2007; revised manuscript received 9 March 2007; published 12 July 2007)

We investigate the quantum Zeno and anti-Zeno effects in spin bath models: the spin-boson model and a spin-fermion model. We show that the Zeno–anti-Zeno transition is critically controlled by the system-bath coupling parameter, the same parameter that determines spin decoherence rate. We also discuss the crossover in a biased system, at high temperatures, and for a nonequilibrium spin-fermion system, manifesting the counteracting roles of electrical bias, temperature, and magnetic field on the spin decoherence rate.

DOI: 10.1103/PhysRevA.76.012109 PACS number(s): 03.65.Xp, 03.65.Yz, 05.30.−d, 31.70.Dk

The quantum Zeno effect (QZE) describes the behavior of a quantum system when frequent short time measurements inhibit decay [1,2]. In some cases, however, the anti-Zeno effect (AZE), namely, an enhancement of the decay due to frequent measurements, is observed [3,4]. The QZE can be easily obtained for an oscillating (reversible) quantum system. When the system is unstable, the situation is more involved, and one can obtain both the QZE and AZE, depending on the interaction Hamiltonian [4], as well as the measurement interval [5]. A crossover from QZE to AZE behavior has been observed in an unstable trapped cold atomic system via a tuning of the measurement frequency [6]. Recently, Maniscalco *et al.* [7] have theoretically investigated the Zeno–anti-Zeno crossover in a model of a damped quantum harmonic oscillator. These authors demonstrated the crucial role played by the short time behavior of the environmentally induced decoherence.

In this paper we focus on spin-bath models, paradigms of quantum dissipative systems, and analyze the conditions for the occurrence of the Zeno and anti-Zeno effects. On a related model, Gurvitz *et al.* [8] have recently demonstrated that there is no Zeno paradox for a qubit interacting with its environment and a detector, which is explicitly included in the model. In other words, measurements can never fully localize a spin when relaxation due to the environment is taken into account. What is then the meaning of the QZE in quantum dissipative models? We define the effect as follows: Instead of focusing on the strict $\tau \to 0$ limit (τ is the measurement interval) we analyze the phenomenology of the decay at times $\omega_c \tau \sim 1-10$, where ω_c^{-1} is the memory time of the bath fluctuations. We demonstrate that depending on the system-bath coupling, the spin decay rate can either decrease with decreasing τ, which we refer to as the Zeno effect or *increase* for more frequent measurements, which we define as the anti-Zeno effect. At the strict $\tau \to 0$ limit a careful inclusion of the measurement apparatus should yield the results of Ref. [8].

Based on analytical derivations and numerical simulations, we find that the crossover between the two processes is critically controlled by the system-bath dimensionless coupling strength, as well as the temperature and the energy bias between the spin states. Specifically, for a spin coupled to a harmonic reservoir at zero temperature the Zeno–anti-Zeno transition and the coherent-incoherent transition of the population dynamics occur exactly at the same system-bath coupling strength. We also analyze the Zeno effect for out-of-equilibrium, electrically biased, situations, and demonstrate that a voltage drop across the junction affects the Zeno behavior as an effective temperature. Our main conclusion is that the same parameters which determine the extent of quantum coherence for the transient population variable, also control the Zeno–anti-Zeno transition. Therefore, the nature of spin decoherence might be predicted from the Zeno dynamics.

The models of interest here are the spin-boson model and a nonequilibrium steady state spin-fermion model, which is a simplified variant of the Kondo model, both are prototype models for understanding dissipation in quantum systems. The spin-boson model, describing a two-level system coupled to a bath of harmonic oscillators, is one of the most important models for elucidating the effect of environmentally controlled dissipation in quantum mechanics [9]. In spite of the model apparent simplicity, it exhibits a very rich behavior. The Kondo model, possibly the simplest model of a magnetic impurity coupled to an environment, describes the coupling of a magnetic atom to the conduction band electrons [10]. This system has recently regained enormous interest due to significant experimental progress in mesoscopic physics [11]. For both models the prototype Hamiltonian includes three contributions

$$H = H_S + H_B + H_{\mathrm{SB}}. \tag{1}$$

The spin system includes a two level system (TLS) with a bare tunneling amplitude Δ and a level splitting B,

$$H_S = \frac{B}{2}\sigma_z + \frac{\Delta}{2}\sigma_x. \tag{2}$$

In what follows we refer to the bias B as a magnetic field in order to distinguish it from potential bias in the nonequilibrium system. In the bosonic case the thermal bath includes a set of independent harmonic oscillators, and the system-bath interaction is linear in the oscillator coordinates

$$H_B^{(b)} = \sum_j \epsilon_j b_j^\dagger b_j,$$

$$H_{\mathrm{SB}}^{(b)} = \sum_j \frac{\lambda_j}{2}(b_j^\dagger + b_j)\sigma_z. \tag{3}$$

Here $b_j^\dagger, b_j$ are bosonic creation and annihilation operators, respectively. In a fermionic model the bath Hamiltonian and the system-bath interaction are given by

$$H_B^{(f)} = \sum_k \epsilon_k a_{k,n}^\dagger a_{k,n},$$

$$H_{\mathrm{SB}}^{(f)} = \sum_{k,k',n,n'} \frac{V_{k,n;k',n'}}{2} a_{k,n}^\dagger a_{k',n'}\sigma_z. \tag{4}$$

Here $a_k^\dagger, a_k$ are fermionic creation and annihilation operators, and the spin interacts with n reservoirs. We also define two auxiliary Hamiltonians $H_\pm$ as

$$H_\pm = \pm\frac{B}{2} + H_{\mathrm{SB}}(\sigma_z = \pm) + H_B. \tag{5}$$

Note that the Hamiltonian (1) does not include explicitly the measuring device. While in Refs. [12] (boson bath) and [13] (fermion bath) the reservoirs serve as continuous detectors, here they are part of the dynamical system under measurement.

Before studying the Zeno behavior of the dissipative systems, we briefly review the results for an isolated TLS. For zero magnetic field, the probability to remain in the initial prepared state is given by $W(t)=\cos^2(\Delta t/2)$ $(\hbar=1)$. The short-time dynamics $(\Delta t \ll 1)$ can be approximated by $W(t) \sim 1-(\Delta/2)^2 t^2$. If measurements are performed at regular intervals τ, the survival probability at time $t=n\tau$ becomes

$$W(\tau)^n = W(t) \sim 1 - n(\Delta/2)^2\tau^2 \sim \exp(-\Delta^2\tau t/4). \tag{6}$$

At short times an effective relaxation rate is identified as

$$\gamma_0(\tau) = (\Delta/2)^2\tau. \tag{7}$$

As τ goes to zero, decay is inhibited, and the dynamics is frozen. This is the quantum Zeno effect. For a rigorous derivation see Ref. [14].

We consider next the influence of the environment on this behavior. Within perturbation theory the dynamics of a TLS coupled to a general heat bath is given as a power series of Δ terms $W(t)=\Sigma_{n=0}^{\infty}\left(\frac{\Delta}{2}\right)^{2n}\Phi_n(t)$ [15]. We have numerically verified that for $\omega_c\tau \lesssim 20$ (ω_c is the reservoir cutoff frequency [16]), the series can be approximated by the first two terms

$$W(\tau) \sim 1 - 2\,\mathrm{Re}\left(\frac{\Delta}{2}\right)^2 \int_0^\tau dt_1 \int_0^{t_1} dt_2 K(t_2),$$

$$K(t) = \langle e^{-iH_+t} e^{iH_-t}\rangle, \tag{8}$$

even for strong system-bath coupling [17], provided that $\Delta\tau < 1$ [18]. Here Re denotes the real part, the Hamiltonians $H_\pm$ are defined in Eq. (5), and the trace is done over the bath degrees of freedom, irrespective of the statistics. Similarly to the isolated case, we can identify an effective decay rate at short times

$$\gamma(\tau) = \frac{2}{\tau}\left(\frac{\Delta}{2}\right)^2 \mathrm{Re}\int_0^\tau dt_1 \int_0^{t_1} K(t')dt'. \tag{9}$$

In deriving Eq. (9) we have assumed that the system-bath density matrix factorizes at all times, and that the bath is kept in thermal equilibirum. These assumptions can be justified at short times, since even at strong coupling, second order perturbation theory, and therefore the factorization of the density matrix, holds [19,20].

In the standard definition of the QZE, the behavior of the effective decay rate (9) with respect to the Markovian rate γ_M identifies the occurrence of the Zeno or anti-Zeno effects [7]. In contrast, in what follows we use the following qualitative definition: The QZE takes place when the population decay rate decreases when τ becomes smaller, while a system for which the decay rate increases for smaller τ, i.e., measurements enhance the decay, shows the AZE. The occurrence of a maxima in $\gamma(\tau)$ is an indication for Zeno–anti-Zeno transition. Our definition for the Zeno and anti-Zeno effects is therefore based on the local properties of the decay rate, while the standard classification is based on the fixed, natural decay. We use this local time definition for practical reasons, since the exact long time decay rates in the spin-boson model and the spin fermion model are not known for general temperature, bias and coupling conditions [21]. For convenience, we also disregard the multiplicative factor $(\Delta/2)^2$ in Eq. (9), which has no effect on the location of the Zeno–anti-Zeno crossover.

The basic question to be addressed in this paper is how does this relaxation rate depend on the system bath coupling. It is clear that when the system is decoupled from the environment, Eq. (9) reproduces the result of the isolated system, Eq. (7). For a dissipative system the central object of our calculation is therefore the correlation function $K(t)$ defined in Eq. (8). For the bosonic system (3), a standard calculation yields [22]

$$K_b(t) = e^{-iE_s t}\exp\left\{-\frac{1}{\pi}\int_0^\infty d\omega \frac{J(\omega)}{\omega^2}[(n_\omega+1)(1-e^{-i\omega t}) + n_\omega(1-e^{i\omega t})]\right\}. \tag{10}$$

Here $n_\omega=[e^{\beta\omega}-1]^{-1}$ is the Bose-Einstein distribution function, $\beta=1/T$ is the inverse temperature, and $E_s=B+\int\frac{J(\omega)}{\pi\omega}d\omega$ is the polaron shift. The spectral density $J(\omega)$ includes the information about the system-bath interaction, $J(\omega)=\pi\Sigma_j\lambda_j^2\delta(\omega-\omega_j)$. For an Ohmic model, $J(\omega)=2\pi\xi\omega e^{-\omega/\omega_c}$, and at low temperatures, $\beta\omega_c \gg 1$, Eq. (10) becomes [23]

$$K_b(t) = \left(\frac{1}{1+i\omega_c t}\right)^{2\xi}\left[\frac{\left(\frac{\pi t}{\beta}\right)}{\sinh\left(\frac{\pi t}{\beta}\right)}\right]^{2\xi} e^{-iE_s t}, \tag{11}$$

where ξ is a system-bath dimensionless coupling parameter [9] that can take values larger than zero. Practically, we limit ourselves to the regime $\xi<1$ for several reasons. (i) The

factorization of the density matrix to its system-bath components becomes questionable for very strong coupling. (ii) In the absence of measurements and at zero temperature the spin system is localized for $\xi \geqslant 1$ [9]. Therefore, in this regime measurements do not affect the system in a trivial way. (iii) Since the Zeno–anti-Zeno transition takes place at $\xi=\frac{1}{2}$ (see discussion below), we focus on the dynamics around this value.

At zero temperature and for zero magnetic field, disregarding the energy shift, the effective decay rate (9) is given by $\left(\xi \neq \frac{1}{2}, 1\right)$

$$\gamma(\tau) = \frac{1-(1+\omega_c^2\tau^2)^{1-\xi}\cos[2(1-\xi)\mathrm{atan}(\omega_c\tau)]}{\tau\omega_c^2(1-\xi)(1-2\xi)}. \quad (12)$$

The limiting short time and long time behavior of this expression is

$$\gamma(\tau) \propto \begin{cases} \tau, & \omega_c\tau \ll 1, \\ \tau^{1-2\xi}, & \omega_c\tau \gg 1, \end{cases} \quad (13)$$

with a crossover taking place at $\omega_c\tau \sim 1$. Therefore, while at short times ($\omega_c\tau \ll 1$) the system always shows the QZE [24], irrespective of the system-bath coupling, at longer times $1/\omega_c < \tau < 1/\Delta$ the qualitative behavior of the decay rate crucially depends on the dimensionless coupling coefficient: the decay is inhibited (QZE) for $\xi < \frac{1}{2}$ and accelerated (AZE) for $\xi > \frac{1}{2}$. At $\xi=\frac{1}{2}$ the decay rate does not depend on the measurement interval

$$\gamma(\tau) \xrightarrow{\ln(\omega_c\tau)/\omega_c\tau<1} \frac{\pi}{\omega_c}. \quad (14)$$

Correspondingly, at zero temperature an unbiased spin oscillates coherently at $\xi=0$, shows damped coherent oscillation for $0<\xi<\frac{1}{2}$, and decays incoherently at strong dissipation, $\frac{1}{2}<\xi<1$. At the crossover value $\xi=\frac{1}{2}$ the system can be mapped onto the Toulouse problem, describing an impurity coupled to a Fermi bath with a constant density of states. This leads to a purely Markovian exponential decay which is unaffected by measurements [25]. We therefore find that the dimensionless coupling constant ξ which controls the extent of spin decoherence, determines the occurrence of the QZE and the AZE.

In addition to the occupation probability $W(t)$, the symmetrized equilibrium correlation function $C(t)$ is also of interest. It is unclear whether the coherent-incoherent transition of this quantity occurs at $\xi=\frac{1}{2}$ [26], similarly to the behavior of the levels population, or below, at $\xi=\frac{1}{3}$ [27]. Yet, since the short-time dynamics of the two-spin correlation function $C(t)$ is controlled by the same function $K_b(t)$ [Eq. (8)] [28], its Zeno–anti-Zeno behavior exactly corresponds with $W(t)$, and thus rigorously undergoes a Zeno–anti-Zeno transition at $\xi=\frac{1}{2}$.

Figure 1 depicts the decay rate $\gamma(\tau)$ for $\xi=0.1-1$. While at short times, $\omega_c\tau<1$, the QZE dominates, at long enough times (specifically here for $\omega_c\tau>2$), the system shows the AZE at strong couplings. The inset manifests that the crossover from the QZE to the AZE occurs at $\xi=\frac{1}{2}$. The transition between the Zeno and anti-Zeno regimes can be manipulated

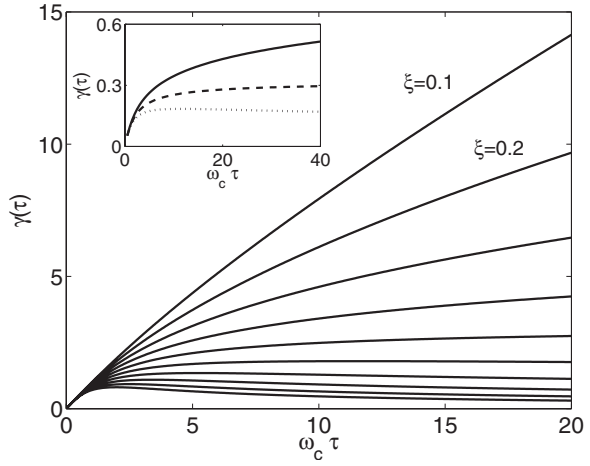

FIG. 1. The effective decay rate for a spin coupled to a bosonic bath at zero temperature for $\omega_c=1$, $E_s=0$, $\xi=0.1, 0.2, 0.3, \ldots, 1$, top to bottom. The appearance of a maximum point in $\gamma(\tau)$ at $\omega_c\tau \sim 1$ for $\xi > 1/2$ marks the transition from QZE to AZE. The inset depicts the rate for $\xi=0.4$ (full), 0.5 (dashed), 0.6 (dotted), $\omega_c=10$. The decay rate $\gamma(\tau)$ in Figs. 1 and 2 is given in units of ω_c^{-1}. In order to reach the appropriate energy units, the data should be multiplied by $\Delta^2/4$.

by applying a finite magnetic field and by employing a finite temperature bath. Figure 2 shows that at weak coupling, a biased system $B/\omega_c \sim 1$ tends toward a pronounced anti-Zeno behavior, in contrast to the zero magnetic field case. The influence of finite temperatures is radically different (inset): It drives the system into the Zeno regime, for all coupling strengths. This can be deducted from Eq. (11): When $\omega_c\tau > 1$, even at low temperatures, $\beta\omega_c \sim 5-10$, the correlation function roughly decays exponentially, $K_b(t) \sim e^{-2\pi\xi t/\beta}$. The resulting decay rate is proportional to τ at short times, saturating at $\omega_c\tau > 1$. We therefore conclude that for a fixed measurement interval τ, modulations in magnetic field and temperature may lead to transitions from a Zeno behavior, to the anti-Zeno effect and vice versa, similarly to the behavior

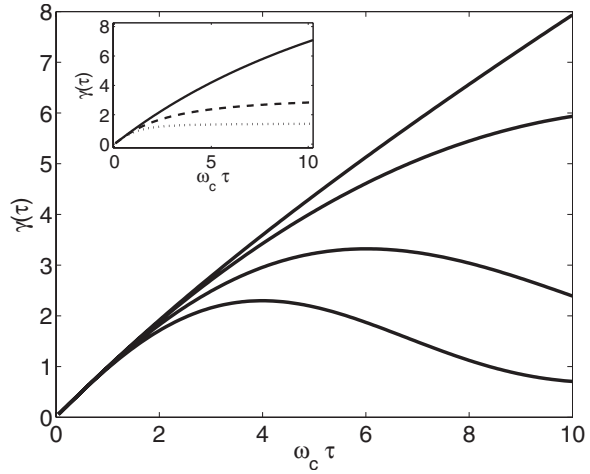

FIG. 2. The Zeno–anti-Zeno transition of a spin-boson model under a magnetic field $T=0$ K, $\omega_c=1$, $\xi=0.1$, $B=0$, 0.2, 0.4, 0.6, top to bottom. Inset: Temperature effect, eliminating the AZE, $\beta\omega_c=5$, $B=0$, $\xi=0.1$ (full), $\xi=0.4$ (dashed), $\xi=0.7$ (dotted).

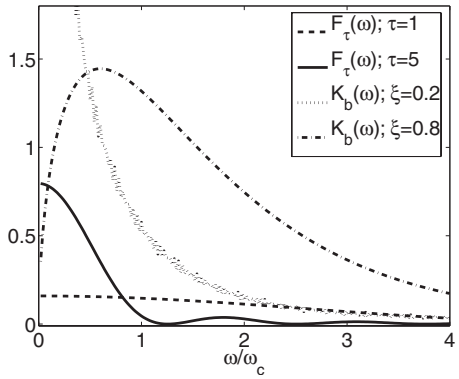

FIG. 3. The QZE and the AZE, as observed through the spectral functions $K_b(\omega)$ and $F_\tau(\omega)$ for a bosonic model with $T=0$, $\omega_c=1$, $E_s=0$ [see Eq. (15) and text below for definitions]. Upon increasing ξ, $K_b(\omega)$ shifts toward higher frequencies overlapping poorly with $F_{\tau=5}(\omega)$, and strongly with $F_{\tau=1}(\omega)$, which leads to the AZE.

observed for the damped harmonic oscillator model, Ref. [7].

Our results can be elucidated by recasting the decay rate as a convolution of two memory functions

$$\gamma(\tau) = 2\int_0^\infty d\omega K(\omega) F_\tau(\omega), \tag{15}$$

where the measurement function is given by $F_\tau(\omega) = \frac{\tau}{2\pi}\mathrm{sinc}^2\left[\frac{(\omega-E_s)\tau}{2}\right]$, and $K(\omega)=\mathrm{Re}\int_0^\infty e^{i\omega t}K(t)dt$, can be interpreted as the reservoir coupling spectrum [4]. Note that $K(t)$ is redefined here without the energy shift. The short-time behavior is therefore determined by the overlap of these two memory functions. For $|E_s-\omega_m| \gg 1/\tau$, with ω_m as the central frequency of $K(\omega)$, AZE takes place, while for a bath with narrow coupling spectrum and for $|E_s-\omega_m| \ll 1/\tau$ the QZE occurs [4]. Note that Eq. (15) holds for a general dissipative system, irrespective of the reservoir statistics.

For the bosonic model, using Eq. (11), Fig. 3 displays the correlation function $K_b(\omega)$ at two values: $\xi=0.2$ (weak coupling) and $\xi=0.8$ (strong coupling). We also show the measurement function $F_\tau(\omega)$ for $\omega_c\tau=1$, 5. We find that at weak coupling, the overlap between these two functions decreases upon shortening τ, leading to the QZE. In contrast, at strong coupling, since the central frequencies of $F_\tau(\omega)$ and $K_b(\omega)$ are detuned, increasing the width of $F_\tau(\omega)$ enhances the overlap between the functions, therefore the decay rate, leading to the AZE. This is clearly seen mathematically: At zero temperature $K_b(\omega)=\frac{1}{\omega_c\Gamma(2\xi)}\left(\frac{\omega}{\omega_c}\right)^{2\xi-1}e^{-\omega/\omega_c}$, with $\omega_m \sim (2\xi-1)\omega_c$. Here $\Gamma(x)$ is the complete Gamma function. This argument also explains the AZE observed at weak coupling for finite magnetic fields. Since $F_\tau(\omega)$ is centered around the bias B, and $\omega_m \sim 0$ for $\xi \leqslant 0.5$, the AZE is expected to prevail for $B\tau > 1$, in agreement with Fig. 2.

We turn now to the fermionic bath. For a *single* reservoir at zero temperature, the fermionic correlation function can be calculated in the context of the x-ray edge singularity problem as $(Dt > 1)$ [29]

$$K_f(t) \sim \frac{e^{-iBt}}{(1+iDt)^{\delta^2/\pi^2}}. \tag{16}$$

Here $\delta=2\,\mathrm{atan}(\pi\rho V/2)$is the scattering phase shift for a constant coupling model $V_{k,k'}=V$, with ρ as the density of states. The energy D is of order of the Fermi sea bandwidth, the analog of the cutoff frequency ω_c in the bosonic case. We have disregarded the energy shift coming from the diagonal coupling $V_{k,k}$, as it can always be accommodated into the external magnetic field B.

Comparing Eq. (16) to the bosonic expression (11), leads to the conclusion that an unbiased spin coupled to a fermionic bath can only manifest the QZE: Since the phase shift cannot exceed $\pi/2$, the exponent in Eq. (16) is always $\leqslant 1$, while according to Eq. (13), the AZE takes place only for larger values which are prohibited in this case. A spin coupled to more than a single lead may attain a larger exponent, which can lead to the AZE [30].

The nonequilibrium spin-fermion system, where the spin couples to *two* fermionic baths with chemical potentials shifted by $\delta\mu$, is much more interesting and involved. In this case we numerically calculate the correlation function $K_f(t)$, since its analytic form is not known at short times $Dt \leqslant 1$ and for arbitrary voltages [31,32]. This is done by expressing the zero temperature many body average as a determinant of the single particle correlation functions [22]

$$K_f(t) = \langle e^{-iH_+t}e^{iH_-t}\rangle = \det[\phi_{k,n;k',n'}(t)]_{k<k_f^n;k'<k_f^{n'}},$$

$$\phi_{k,n;k',n'}(t) = \langle k,n|e^{-ih_+t}e^{ih_-t}|k',n'\rangle. \tag{17}$$

Here $H_\pm=\Sigma h_\pm$, where $h_\pm$ are the single particle Hamiltonians for the individual conduction electrons, $|k,n\rangle$ are the single particle eigenstates of $H_B^{(f)}$, and the determinant is evaluated over the occupied states. k_f^n is the Fermi energy of the nth reservoir. For a short-time evolution, it is satisfactory to model the fermionic reservoirs using $\sim$200 states per bath, where bias is applied by depopulating one of the reservoirs with respect to the other. We have also utilized a Lorentzian density of states of width Γ, with tails that are long enough, in order to eliminate artificial reflections from the boundaries at the relevant times, see inset of Fig. 4. As a specific model we assume constant nondiagonal couplings $V_{k,n;k',n'}=V$; $(n \neq n')$, while diagonal interactions are omitted, $V_{k,n;k',n}=0$.

The decay rate $\gamma(\tau)$, Eq. (9), is presented in the main plot of Fig. 4 for three situations: In the absence of both magnetic field and electric bias (full), including a finite magnetic field (dashed), and under an additional potential bias (dotted). We find that the potential bias in the fermionic system plays the role of the temperature in the bosonic environment [32], driving the anti-Zeno effect into a Zeno behavior.

Summarizing our observations, we find that the same coupling parameter that monitors spin decoherence and relaxation, determines the Zeno behavior. In addition, while finite temperatures and electric bias eliminate the AZE, applying a finite magnetic field can revive the effect. The relationship between the Zeno effect and spin dynamics also implies on the feasible *control* over the environment induced spin deco-

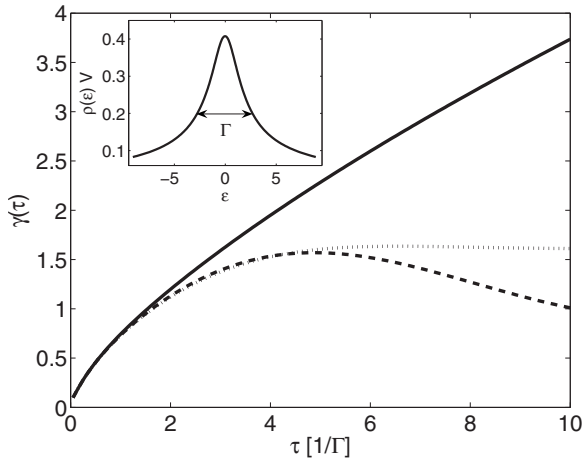

FIG. 4. The effective decay rate for a spin coupled to two fermionic baths demonstrating the counteracting roles of the magnetic field and electrical bias. $B=0$, $\delta\mu=0$ (full); $B=0.5$, $\delta\mu=0$ (dashed); $B=0.5$, $\delta\mu=0.8$ (dotted). The inset shows the Lorentzian shaped density of states, multiplied by the system-bath coupling strength, with Γ as the full width at half maximum. The decay rate is given in units of Γ^{-1}. In order to obtain the appropriate energy units, the rate constant should be multiplied by the factor $\Delta^2/4$.

herence utilizing the Zeno effect, which is crucial for quantum computing applications [33].

In our theoretical formalism, measurements are simply described using the projection postulate, assuming instantaneous and ideal measurements. In the dynamical formalism, developed, e.g., in Ref. [13], one explicitly includes the interaction with a detector in the calculations, and analyzes the dynamics of the enlarged system. It has recently been shown that these two formalisms produce the same results under some standard conditions, e.g., for a photodetection measurement one should require that every photon is detected with an identical response time [34]. We therefore expect that repeating our derivations while assuming continuous measurements, e.g., using the Bloch-type formalism of Ref. [8], should yield results which comply with our conclusions. The main deviation is expected to appear at very short times: Reference [8] demonstrates that in the presence of relaxations the Zeno paradox does not exist, and the decay rate approaches a constant at $\tau\rightarrow 0$, rather than decay to zero as seen in Figs. 1, 2, and 4.

The transition from Zeno to anti-Zeno behavior can be controlled by modifying the environmental parameters such as the spectral density, temperature, electrical bias, and by changing the system-bath interaction, as well as the spin parameters. Trapped ions in an optical lattice is a highly versatile system possibly capable of showing the Zeno–anti-Zeno crossover. In recent years it has become feasible to trap chains of atoms, to couple them in a controlled way to the oscillatory "phonon" modes of the chain, and to probe them by a laser field [35]. Another possible setup is an atomic Bose-Einstein condensate interacting with a laser field [2]. This system is predicted to give rise to composite quasiparticles: local impurities dresses by (virtual) phonons [36]. The spin-fermion model could be realized in a semiconductor microstructure consisting of two coupled quantum dots, simulating a double-well potential, interacting with a current carrying quantum point contact (QPC) [37]. Measurements of the spin state can be done either continuously with an additional QPC, serving this time as a detector, or using laser radiation, directly detecting the population in each of the wells.

This work was supported by NSF Grant No. (NIRT)-0210426.

[1] B. Misra and E. C. G. Sudarshan, J. Math. Phys. **18**, 756 (1977); D. Home and M. B. A. Whitaker, Ann. Phys. (N.Y.) **258**, 237 (1997).
[2] E. Streed, J. Mun, M. Boyd, G. Campbell, P. Medley, W. Ketterle, and D. Pritchard, Phys. Rev. Lett. **97**, 260402 (2006).
[3] W. C. Schieve, L. P. Horwitz, and J. Levitan, Phys. Lett. A **136**, 264 (1989).
[4] A. G. Kofman and G. Kurizky, Nature (London) **405**, 546 (2000).
[5] P. Facchi, H. Nakazato, and S. Pascazio, Phys. Rev. Lett. **86**, 2699 (2001).
[6] M. C. Fischer, B. Gutierrez-Medina, and M. G. Raizen, Phys. Rev. Lett. **87**, 040402 (2001).
[7] S. Maniscalco, J. Piilo, and K-A Suominen, Phys. Rev. Lett. **97**, 130402 (2006).
[8] S. A. Gurvitz, L. Fedichkin, D. Mozyrsky, and G. P. Berman, Phys. Rev. Lett. **91**, 066801 (2003).
[9] A. J. Legget *et al.*, Rev. Mod. Phys. **59**, 1 (1987).
[10] J. Kondo, Prog. Theor. Phys. **32**, 37 (1964).
[11] G. A. Fiete and E. J. Heller, Rev. Mod. Phys. **75**, 933 (2003).
[12] O. V. Prezhdo, Phys. Rev. Lett. **85**, 4413 (2000).
[13] S. A. Gurvitz, Phys. Rev. B **56**, 15215 (1997); Quantum Inf. Process. **2**, 15 (2003).
[14] B. Kaulakys and V. Gontis, Phys. Rev. A **56**, 1131 (1997).
[15] L.-D. Chang and S. Chakravarty, Phys. Rev. B **31**, 154 (1985).
[16] The fermionic reservoirs are modeled by a Lorentzian density of states with a full width at half maximum Γ. We have verified that Eq. (8) typically holds for $\Gamma\tau\lesssim 50$.
[17] We define "strong system-bath coupling" as $\xi>0.5$ (bosons) and $\pi\rho V\gtrsim 1$ (fermions). These parameters are defined after Eqs. (11) and (16), respectively.
[18] In the discussion below we always assume that $\Delta\tau<1$.
[19] R. Zwanzig, *Nonequilibrium Statistical Mechanics* (Oxford University Press, New York, 2001).
[20] D. Egorova, M. Thoss, W. Domcke, and H. Wang, J. Chem. Phys. **119**, 2761 (2003).
[21] F. Lesage and H. Saleur, Phys. Rev. Lett. **80**, 4370 (1998).
[22] G. D. Mahan, *Many-particle Physics* (Plenum, New York, 2000).
[23] C. Aslangul, N. Pottier, and D. Saint-James, Phys. Lett. **111A**, 175 (1985).
[24] A careful inclusion of a continuous detector shows that when

the TLS interacts with an environment, the measurement cannot localize the spin even when $\tau \to 0$, where $\gamma(\tau)$ approaches a constant [8].

[25] At the Toulouse point the polarization decay rate is $2\pi/\omega_c$ [9], twice our result. At short times our expression for the decay of the upper level population agrees with this value.

[26] J. T. Stockburger and C. H. Mak, Phys. Rev. Lett. **80**, 2657 (1998).

[27] F. Lesage, H. Saleur, and S. Skorik, Phys. Rev. Lett. **76**, 3388 (1996).

[28] M. Sassetti and U. Weiss, Phys. Rev. A **41**, 5383 (1990).

[29] P. Nozieres and C. T. De Dominicis, Phys. Rev. **178**, 1097 (1969).

[30] A spin coupled to three electrodes with equal chemical potentials: source ($n=1$), drain ($n=3$), and a gate ($n=2$), with $V_{k,1;k',3}=V_{k,3;k',1}=V_{k,2;k',2}=V$, else $V_{k,n;k',n'}=0$, acquires the maximal exponent of 3.

[31] T.-K. Ng, Phys. Rev. B **54**, 5814 (1996).

[32] A. Mitra and A. J. Millis, Phys. Rev. B **72**, 121102(R) (2005).

[33] O. Hosten *et al.*, Nature (London) **439**, 949 (2006).

[34] K. Koshino, Phys. Rev. A **71**, 034104 (2005).

[35] I. Bloch, Nat. Phys. **1**, 23 (2005).

[36] I. E. Mazets, G. Kurizki, N. Katz, and N. Davidson, Phys. Rev. Lett. **94**, 190403 (2005).

[37] G. Hackenbroich, B. Rosenow, and H. A. Weidenmuller, Phys. Rev. Lett. **81**, 5896 (1998).